

Determination of Near-Station Crustal Structure and the Regional Seismic Event Location Problem

Lian-She Zhao and Cliff Frohlich
Institute for Geophysics
The University of Texas at Austin
8701 North MoPac
Austin, TX 78759-8397

AFOSR Contract No. F49620-94-1-0287

Since crustal structure strongly influences the character of regional seismic waveforms, a knowledge of near-station crustal structure is necessary for obtaining single-station event locations of small ($M \sim 3$) seismic events. In this study we demonstrate that it is practical to use a receiver-function method for determining near-station crustal structure; then, we then use this structure as a basis for constructing synthetic waveforms, and determine single-station regional event locations by comparing the synthetic and observed waveforms.

Our receiver-function approach for determining crustal structure utilizes vertical-component P-group waveforms from teleseismic events as input for synthesizing a radial-component waveform for a trial, layered, near-station crustal model. Then, we compare the synthetic and observed radial-component waveforms, and change the crustal model until they are sufficiently similar. To improve efficiency we have implemented several features in our software:

- For synthesizing radial-component waveforms from vertical-component data we employ a theoretical approximation which is exact to second order in the reflection and transmission coefficients; thus, we call this second-order, radial-vertical comparison the SORVEC method;
- For synthesizing reverberation waveforms for a n -layer-over-a-halfspace crustal model we show it is generally sufficient to calculate amplitudes for only $(6n+1)$ carefully selected rays;
- To determine crustal structure we have developed an inversion scheme which utilizes a very fast simulated annealing (VFSA) algorithm which is much faster than grid-search methods, Monte-Carlo methods, or ordinary simulated annealing methods.

Using the SORVEC-VFSA algorithm we have determined flat-layered crustal models beneath 12 seismic stations, one (PAS) in California and 11 in Tibet. To locate regional earthquake near individual stations we use the models using data from teleseismic earthquakes situated at similar azimuths, and determine a crustal model possessing up to five layers. However, often the data fit for 5-layer models is not significantly better than for the 4-layer models; usually the optimal 5-layer models possess two adjacent layers with nearly identical shear velocities which were merged in the optimal 4-layer model.

Finally, using these crustal models we demonstrate that it is possible with single-station data to accurately locate earthquakes with magnitudes of ~ 3 which occur at distances of up to a few hundred km. We determine the event-station azimuth from phase polarization, then we compare observed seismograms with synthetics constructed at 1-2 km intervals over a range of distances and depths. For a test event occurring in California, our location determined by fitting waveforms recorded at PAS was virtually identical to the location determined by the California network. For a test event in Tibet our location differed significantly from that reported by the ISC.

19960624 195

OBJECTIVES

Our objective is to develop practical methods for locating small ($M \sim 3$) regional seismic events using single-station waveform data. Our hypothesis is that we can do this by straightforward waveform comparison methods if we know near-station well enough so that we can construct reasonable synthetic waveforms. In this study, we make several practical improvements to a previously-developed receiver function method, and, we determine the optimum three- to five-layer crustal velocity structures beneath a number of three-component broadband seismic stations. We then utilize the crustal structures so found to test how well we can determine event locations from single-station recordings of small ($M \sim 3$) seismic events.

RESEARCH ACCOMPLISHED

Software Development

To locate small seismic events using waveforms recorded at a single seismic station, it is necessary to determine at least three parameters-- these are: 1) the direction of arrival, or azimuth, or the event with respect to the station; 2) the event-to-station distance; 3) the focal depth of the event. Generally different parts of the arriving waveforms are useful for assessing each of these parameters; polarization of the P-group or surface wave group determines the event azimuth; time delays between P, S, and surface wave groups fixes the event distance; while time delays between crustal reverberation phases within the P group provides information about event focal depth. The regional crustal structure-- near the source, along the path, and near the station-- exercises a strong influence on the determination of all these parameters. However, focal depth is usually the most difficult parameter to determine because near-station crustal reverberations may be mistaken for depth phases unless the near-station crustal structure is well known.

Recently, we have been developing practical methods for determining near-station crustal structure using a receiver-function approach (Zhao and Frohlich, 1994; 1995). The essential strategy is to use vertical-component P-group waveforms from teleseismic events as input for synthesizing a radial-component waveform for a trial, layered, near-station crustal model (Figure 1). Then, we compare the synthetic and observed radial-component waveforms, and change the crustal model until they are sufficiently similar. The method is able to determine crustal structure because time-delays and relative amplitudes of radial- and vertical-component phases in the P group coda are strongly affected by the details of near-station crustal layering.

In our software to determine near-station crustal structure we have implemented three features to improve efficiency. First, our scheme for synthesizing and comparing radial-component waveforms from vertical-component data utilizes a theoretical approximation which is exact to second order in the reflection and transmission coefficients; thus, we call this second-order, radial-vertical comparison the SORVEC method. Second, for synthesizing reverberation waveforms for a n -layer-over-a-halfspace crustal model we only calculate the amplitudes for $(6n+1)$ rays (Figure 2). We have performed extensive testing to demonstrate that this provides an adequate fit between data and synthetics for nearly all realistic crustal models; except in pathological cases the $(6n+1)$ rays include all arrivals with amplitudes exceeding 5% of the initial P wave.

Finally, for applying the SORVEC algorithm to determine crustal structure, we have developed an inversion scheme which utilizes a very fast simulated annealing (VFSA) algorithm (Sen and Stoffa, 1991; Zhao et al., 1995). The VFSA inversion is much faster than grid-search

methods, Monte-Carlo methods, or ordinary simulated annealing methods. However, VFSA still retains the ability to find the global optimum crustal model that provides a fit between synthetic and real radial-component data, even though the relationship between crustal structure and data fit is highly nonlinear.

Crustal Models Determined from Teleseismic Waveforms

Using the SORVEC-VFSA algorithm described above, we have determined flat-layered crustal models beneath 12 seismic stations, one (PAS) in California and 11 in Tibet. To determine a crustal model at each station we utilized data from several earthquakes with azimuths similar to those of regional earthquakes of interest. For station PAS we evaluated teleseismic waveforms from four earthquakes in Alaska and the Kuriles and found the optimal crustal model with five layers and a total thickness of 26 km (Figure 3). However, only three layers were significant, as the top layer was exceedingly thin (less than 1/2 km), and the shear velocity in the fifth layer did not differ from that in the fourth layer.

For each station in Tibet teleseismic events were available at a variety of different azimuths, so we evaluated 10 or more teleseismic events to determine optimum "average" models. In Tibet the crustal shear velocity typically possessed of a 1-2 km thick lid with velocity of ~1.8 km/sec overlying a 10-30 km thick layer with velocity of 3.-4.0 km/sec. Beneath this was a lower-velocity layer extending to depths of 40-55 km. Beneath all stations the crust is unusually thick by ordinary standards, as the Moho lay at about 70-80 km depth. Although we evaluated the data to find the best-fitting 3-layer, 4-layer, and 5-layer models for each station, often the data fit for 5-layer models was not significantly better than for the 4-layer cases; usually the optimal 5-layer models possessed two adjacent layers with nearly identical velocities which were merged in the optimal 4-layer model.

Seismic Event Location Using Single-Station Data

We have utilized crustal models determined as described above as a basis for locating small seismic events. In California single-station event location is complicated because the crust possesses considerable lateral heterogeneity. However, because the California network possesses a large number of stations, high-quality, independently-determined locations are generally available for comparison with our single-station locations.

Using the crustal model in Figure 3, we relocated a magnitude 3.1 earthquake which occurred on 8 February 1995 near station PAS. After determining the event-station azimuth from phase polarization, we constructed synthetic seismograms at 2 km intervals over a range of distances and at 1 km intervals over a range of depths (Figure 4). The best fit between these synthetics and the PAS vertical- and radial-component waveforms (Figure 4) occurred for distances of 24-26 km from PAS, and focal depths of 5 km. This was virtually identical to the location determined by the California network. Nevertheless, the fit between data and synthetics is not perfect, especially for the initial P phase, which is nearly absent in the data and quite prominent in the synthetics. The fit is quite good, however, for the surface wave group and for the S group, where several prominent crustal reverberations predicted by the crustal model of Figure 3 are evident.

As a further demonstration of the method we relocate an earthquake with m_b of 4.5 which occurred on 10 August 1991 near station AMDO in Tibet. We first determine the station-event azimuth by finding the azimuth which minimizes the signal energy arriving between the P and the S (Figure 5); note that the back azimuth so found (~35°) is significantly different than that (~15°) for the location reported by the ISC (33.87°N, 92.19°E, $h = 8$ km). Next, we use our

SORVEC-VFSA to determine a crustal structure for AMDO (Figure 6) using a teleseism that occurred on 26 March 1992 in Alaska, chosen because it possessed a similar back azimuth (44°) to the regional event. Finally, using this crustal model we generated synthetics over a range of distances, depths, and focal mechanisms to compare with the vertical and radial waveforms recorded at AMDO for the 10 August 1991 event. The best fit between synthetics and observations occurs for a station-event distance of 190 km and a focal depth of 8 km (Figure 7). While this focal depth is identical to that reported by the ISC, the epicenter differs by about 60 km. Since the closest station used in the ISC location was at a distance 6.6° , we believe that our location is more accurate.

CONCLUSIONS AND RECOMMENDATIONS

- Testing demonstrates that our SORVEC-VFSA algorithm for determining crustal structure from teleseismic waveforms is effective for determining crustal models which consist of three to five flat layers over a halfspace. The algorithm is fast, and generally finds nearly the same optimal crustal model for input data from teleseisms occurring at different azimuths.
- We find that three- or four-layer crustal models generally provide an adequate basis for constructing synthetic seismograms that strongly resemble the waveforms of small-magnitude, real, regional seismic events. We usually are unable to obtain significantly better fits between real and synthetic seismograms by constructing synthetics using crustal models with five or more layers.
- We here test the effectiveness of locating small seismic events with single-station data by determining event-station azimuth from P-group and surface wave polarization, and event-to-station distance and event focal depth by a grid-search comparison of real and synthetic seismograms. In effect this means that event-to-station distance depends on time delays between the P group, S group and surface wave group, while focal depth depends on relative amplitudes and time delays of reverberation phases within the P group. Our preliminary results indicate that using only single-station waveforms we can obtain accurate locations for small events ($M \sim 3$) at distances of ~ 100 km or more.
- These results imply that the crustal models we obtain using teleseismic data and the SORVEC-VFSA method are good representations of regional crustal structure at distances of ~ 100 km or more from the receiving stations. Otherwise it would not be possible to fit waveforms of regional seismic events with synthetics generated using these crustal structures.

References:

- Sen, M. K. and P. L. Stoffa, Nonlinear one-dimensional seismic waveform inversion using simulated annealing, *Geophysics*, 56, 1624-1638, 1991.
- Zhao, L.-S. and C. Frohlich, Crustal and upper mantle velocity structure beneath seismic stations from modeling teleseismic waveforms, *Proceedings, 16th Annual Seismic Research Symposium, Thornwood, New York*, Air Force Office of Scientific Research, 400-406, 1994 PL-TR-94-2217, ADA284667
- Zhao, L.-S. and C. Frohlich, Teleseismic body-waveforms and receiver structures beneath seismic stations, *Geophys. J. Int.*, (submitted, 1995).
- Zhao, L.-S., M. K. Sen, P. Stoffa and C. Frohlich, Application of very fast simulated annealing to the determination of crustal structure beneath Tibet, *Geophys. J. Int.*, (submitted, 1995).

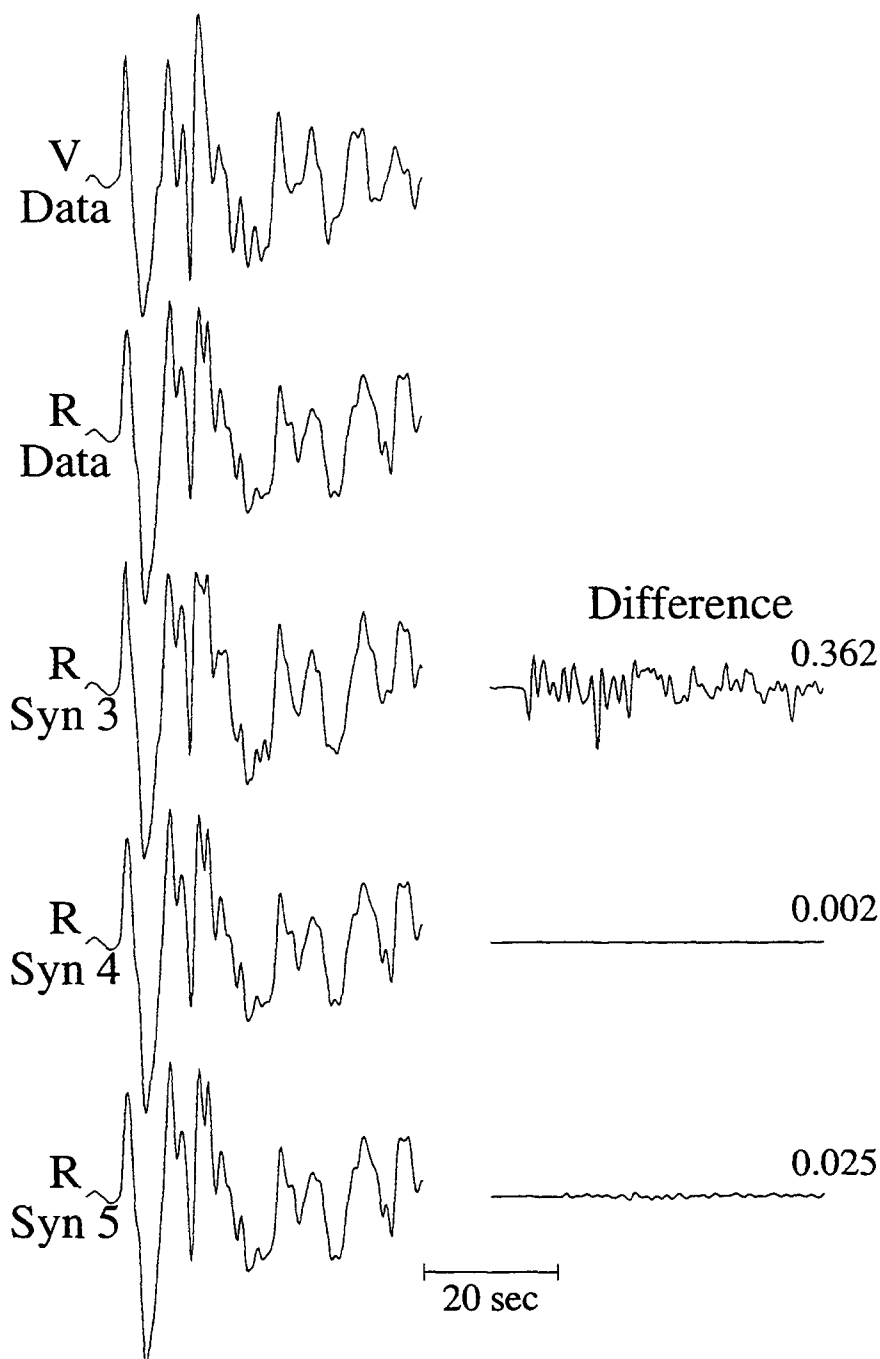


Figure 1. Comparison of radial-component observations with synthetic signals generated for different classes of crustal models with the SORVEC method. Here we use the signal labeled "V" (vertical component of a P wave recorded at station MAQI in Tibet from an earthquake occurring on 17 February 1992) as input for SORVEC to generate a radial-component signal, "R", using the 4-layer-over-halfspace crustal model. Then we test the VFSA inversion method by searching to find the best-fitting crustal models having 3, 4, and 5 layers and the associated radial-component synthetic signals (labeled "Syn 3", "Syn 4" and "Syn 5"). "Difference" column is the difference between the "Radial" signal for the Input crustal structure and the synthetics generated for the best-fitting models; the numbers at right are the misfit, i. e., the amplitude of difference as a fraction of the maximum amplitude of radial component. Note that the 4- and 5-layer models provide excellent fits, whereas the fit for the 3-layer model is significantly poorer.

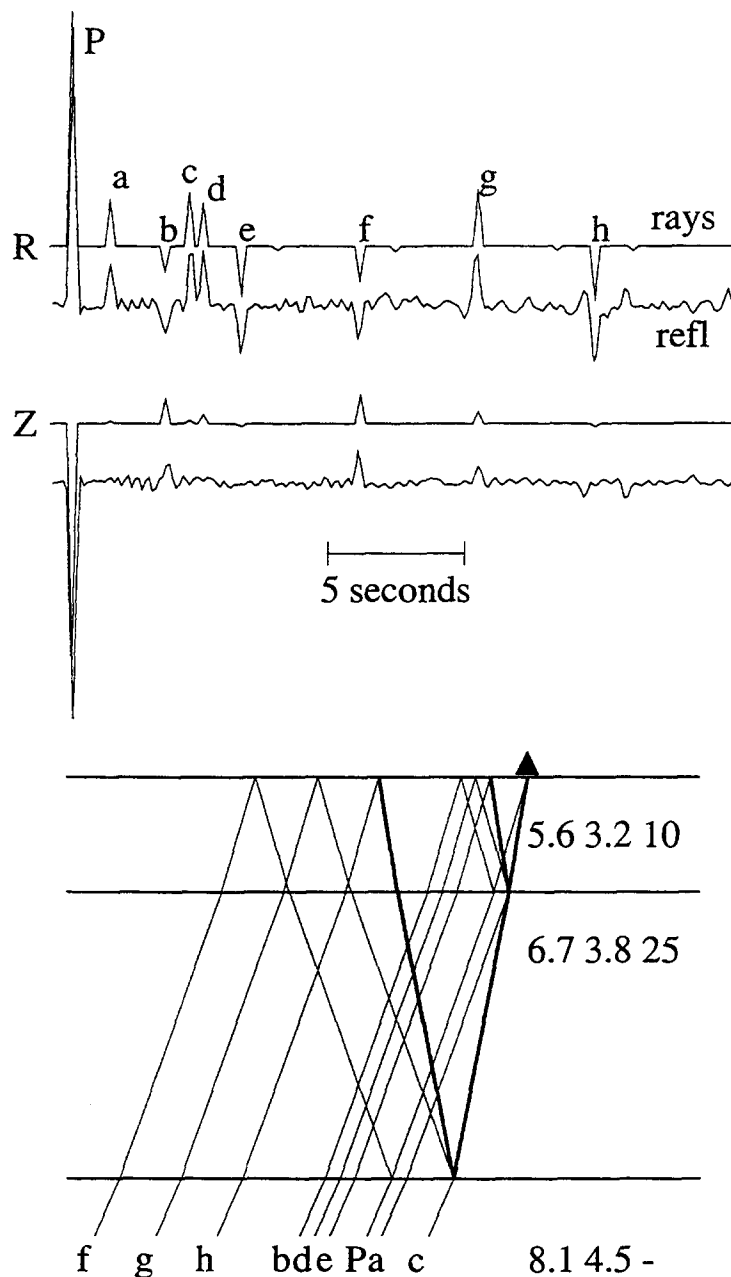


Figure 2. Comparison of radial- (top two traces-- labeled R) and vertical-component (middle two traces-- labeled Z) synthetics generated using generalized ray theory (upper trace in each pair) and with reflectivity (lower trace) for a two-layer-over-a-halfspace model (bottom-- numbers at right represent model P and S velocities and layer thicknesses). Only the nine rays with the labeled ray paths have significant energy.

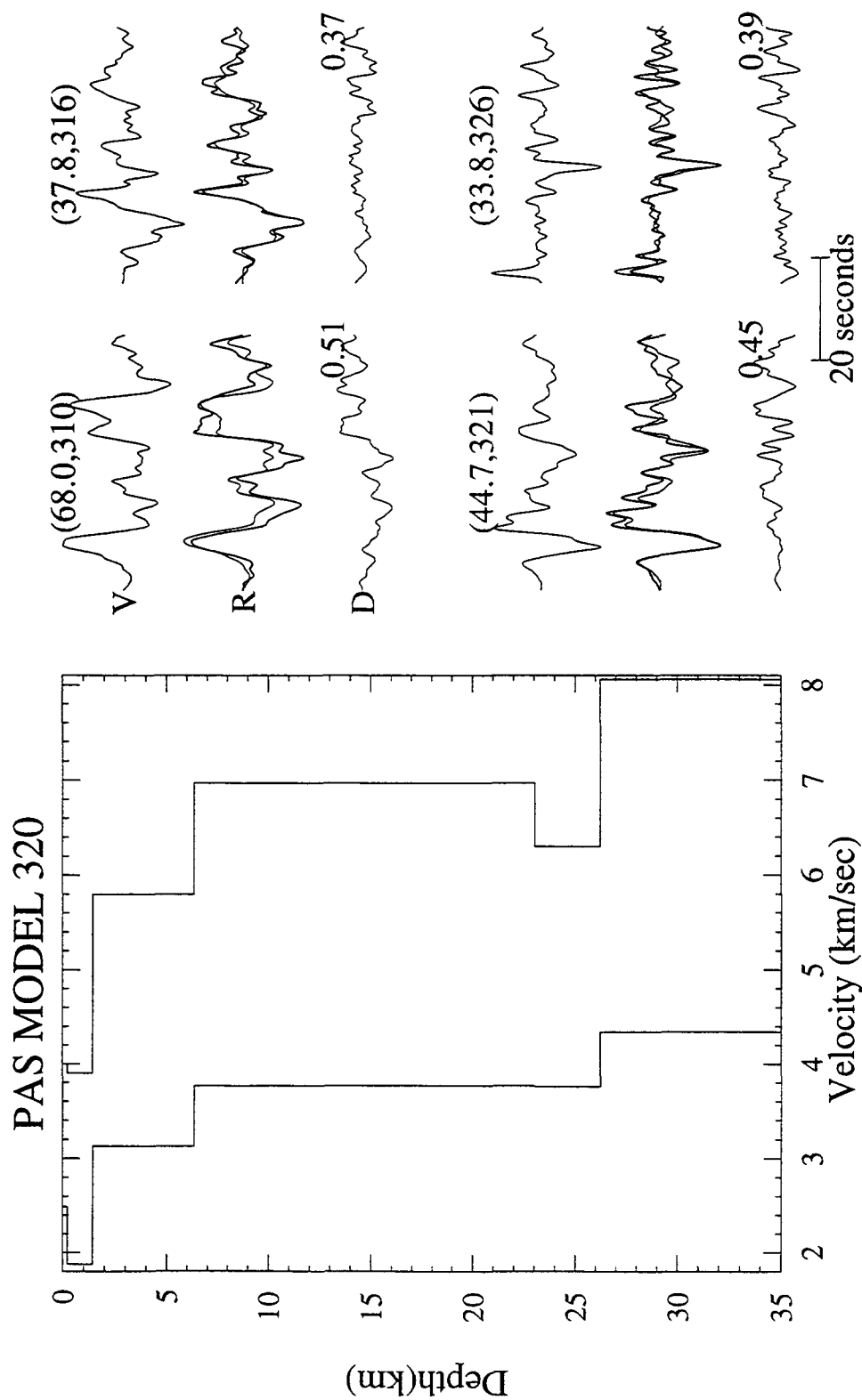


Figure 3. (Left panel) Optimal 5-layer crustal model determined with our SORVEC-VFSA algorithm for station PAS (Pasadena, California). Note that the topmost layer is very thin ($< 1/2$ km), and that the shear velocity in the fifth layer is indistinguishable from the velocity in the fourth layer. Right panel shows fit between telescismic waveforms and synthetics generated using the model at left.

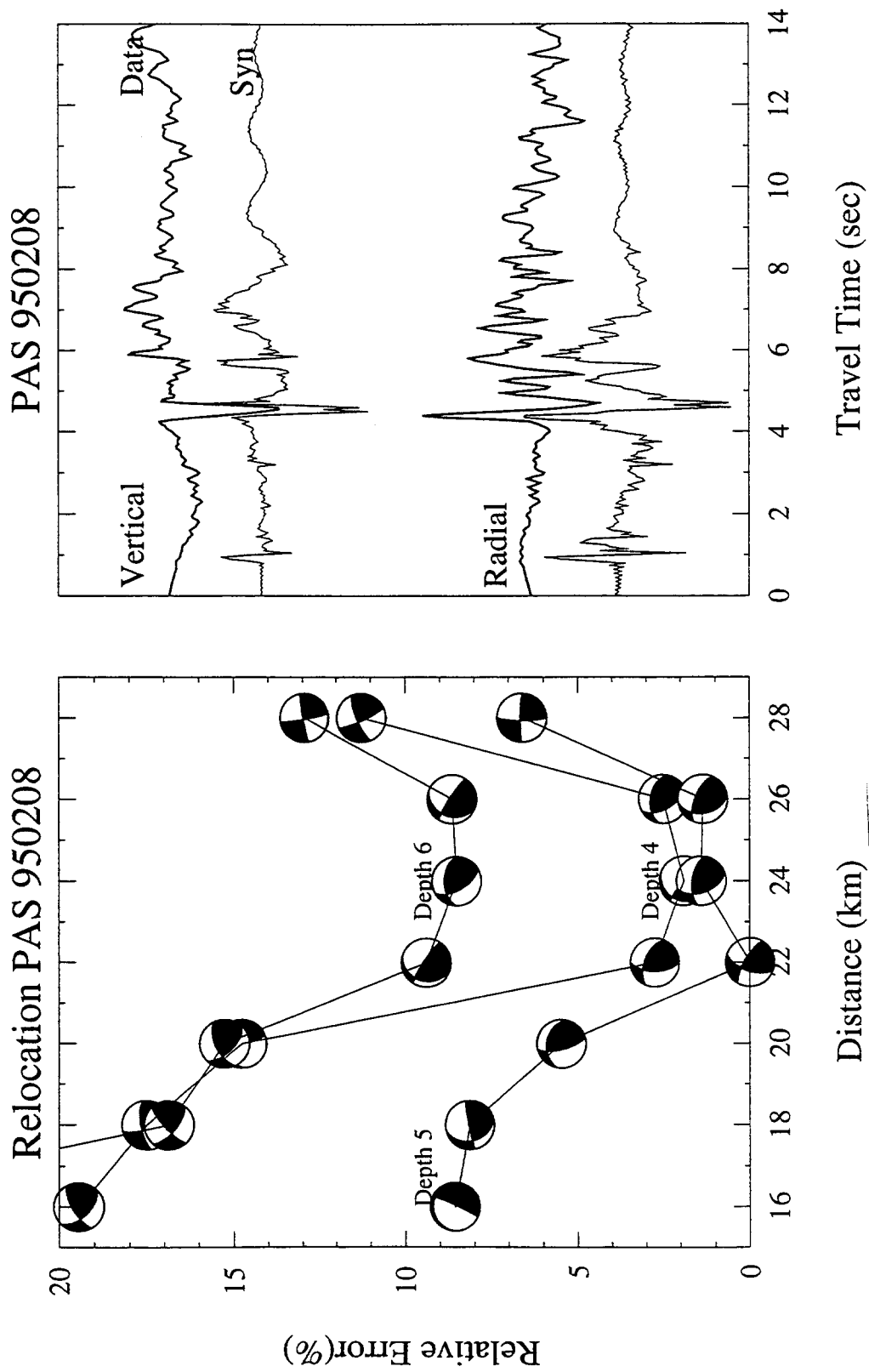


Figure 4. (Left panel) How station-event distance and event focal depth influence fit between data and synthetic waveforms at PAS for the earthquake of 8 Feb. 1995. Relative error is the percentage difference between a normed fit and the optimum fit (0% relative error); best fitting focal mechanism is determined by a grid search for each trial distance and focal depth as indicated by plotted beach-fitting mechanism. (Right panel) Comparison of vertical- and radial-component waveforms at PAS (upper traces) with best-fitting synthetics (lower traces).

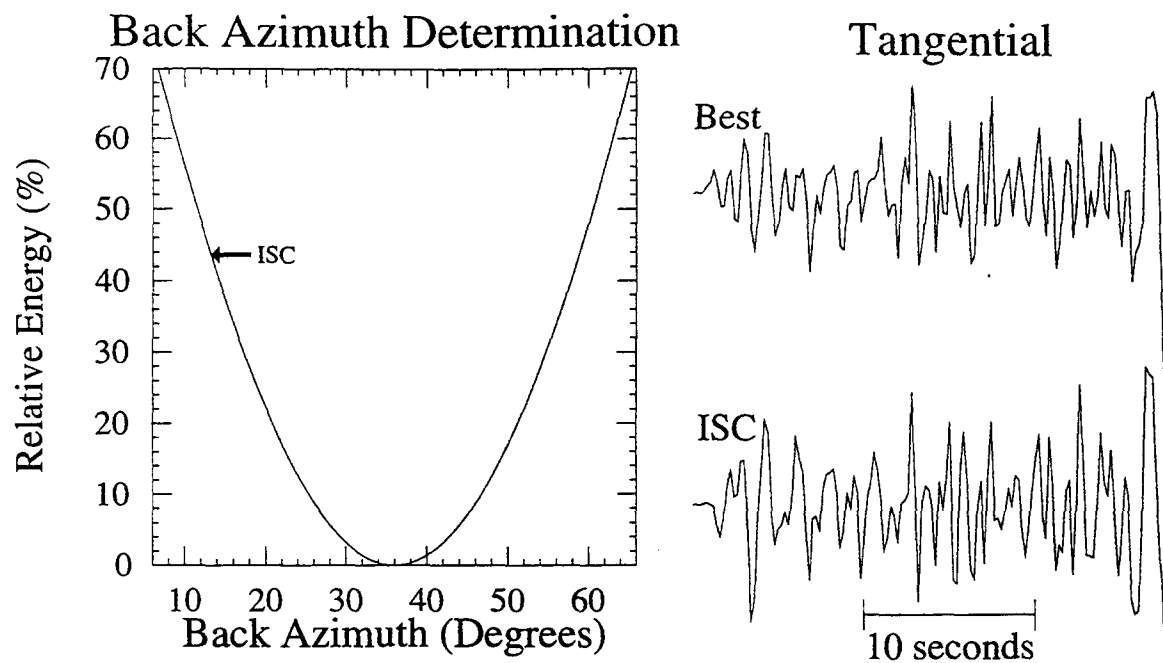


Figure 5. (Left panel) Dependence of tangential-component energy of P-group phases on back azimuth chosen for direction of arrival. Earthquake occurred 10 August 1991; station is AMDO in Tibet; energy is determined for the 30 seconds of signal following the initial P arrival. Note that minimum energy occurs for a back azimuth of 35°, while energy is 45% greater for back azimuth corresponding to location reported by the ISC. Right panel shows the tangential-component waveforms for the smallest-energy (top) and ISC-reported (bottom) azimuths.

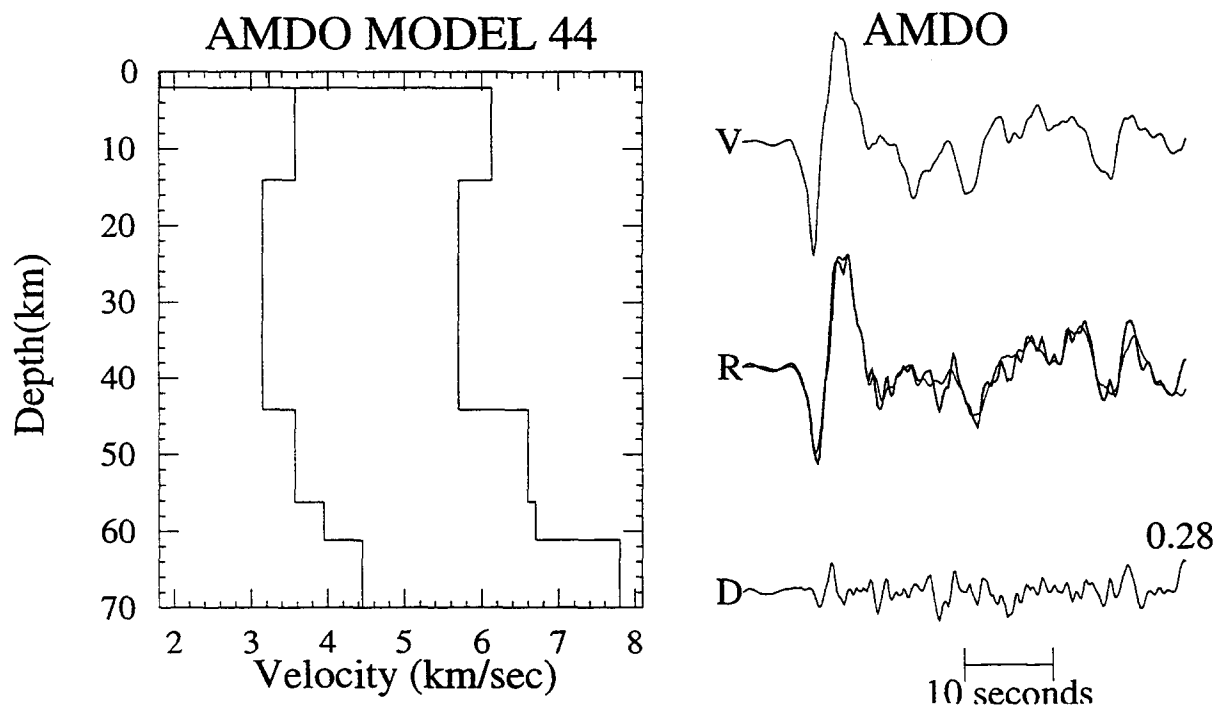


Figure 6. (Left panel) Optimum five-layer crustal model determined by the SORVEC-VFSA algorithm for station AMDO in Tibet using waveforms from an earthquake occurring in Alaska on 26 March 1992. (Right panel) Vertical- (V) and radial-component (R) waveforms for this earthquake recorded at AMDO (light lines), and synthetic radial-component waveform (dark line) for the optimum crustal model at left. Trace "D" is the difference between observed and synthetic radial-component waveforms.

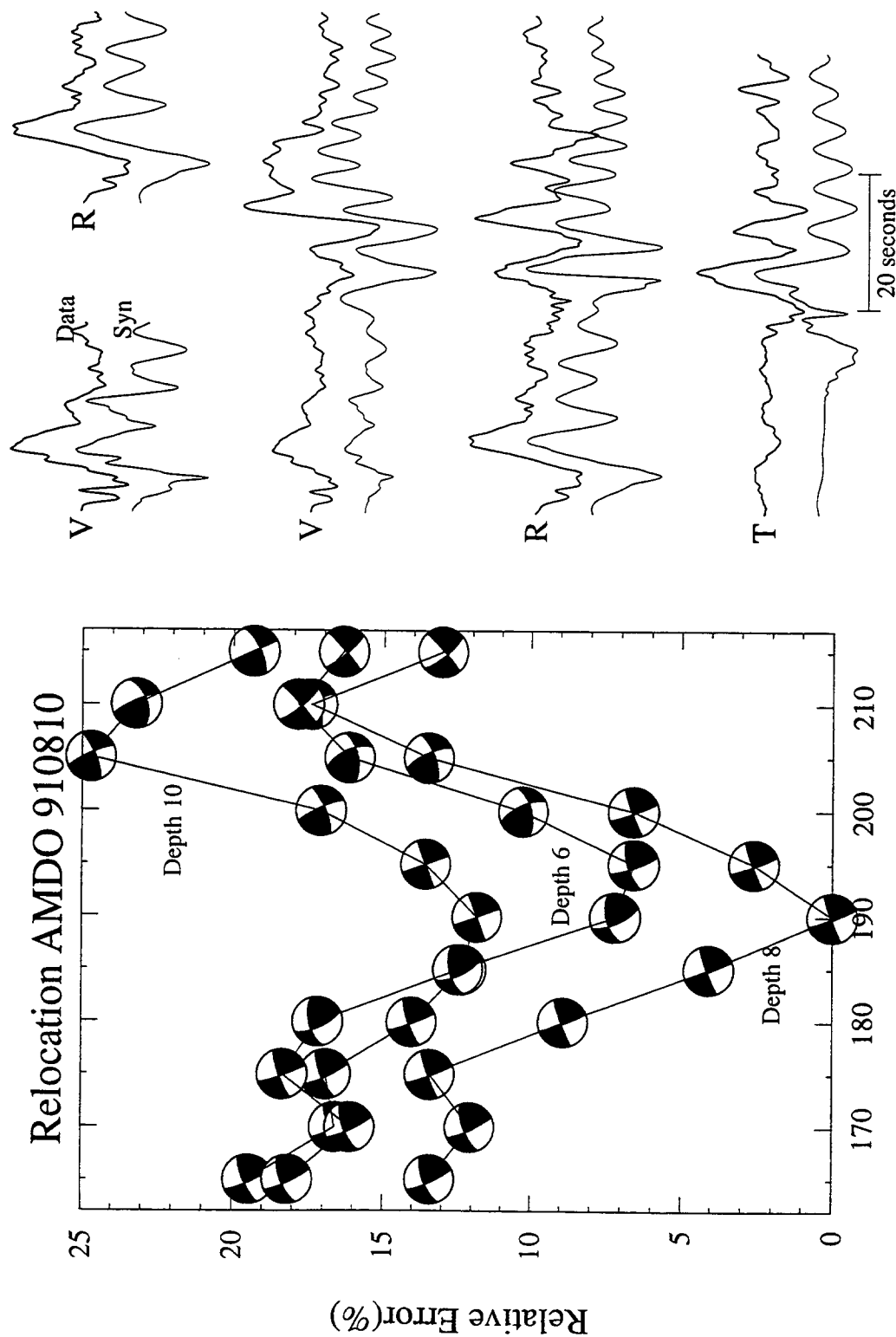


Figure 7. (Left panel) Relative error (i. e., misfit) between observed waveforms and synthetics generated for a range of distances and depths. The earthquake is the regional event of 10 August 1991, and synthetics assume the crustal model of Figure 6; best fitting focal mechanism is determined by a grid search for each trial distance and focal depth as indicated by plotted beach-ball mechanism. (Right panel) Comparison of vertical- (V), radial- (R), and tangential-component (T) waveforms for data (top trace) and synthetics (bottom trace) generated for the best-fitting distance, depth, and focal mechanism as determined in the left panel.